Critical aspects in occupational exposure assessment with different aerosol metrics in an industrial spray coating process

Franco Belosi [a], Antti Joonas Koivisto [b,c,d], Irini Furxhi [e,f], Jesús Lopez de Ipiña [g], Alessia Nicosia [a], Fabrizio Ravegnani [a], Simona Ortelli [h,*], Ilaria Zanoni [h], Anna Costa [h]

[a] CNR-ISAC, National Research Council of Italy, Institute of Atmospheric Sciences and Climate, Via Gobetti 101, 40129 Bologna, Italy
[b] Air Pollution Management APM, Mattilanmäki 38, 33610 Tampere, Finland
[c] Institute for Atmospheric and Earth System Research (INAR), University of Helsinki, PL 64, FI-00014 UHEL, Helsinki, Finland
[d] ARCHE Consulting, Liefkensstraat 35D, Wondelgem B-9032, Belgium
[e] Transgero Limited, Cullinagh, Newcastle West, Co. Limerick, Limerick, Ireland
[f] Department of Accounting and Finance, Kemmy Business School, University of Limerick, Limerick V94 T9PX, Ireland
[g] TECNALIA, Basque Research and Technology Alliance (BRTA), Parque Tecnológico de Alava, Leonardo Da Vinci 11, 01510 Miñano, Spain
[h] CNR-ISSMC (former ISTEC), National Research Council of Italy, Institute of Science, Technology and Sustainability for Ceramics, Via Granarolo 64, 48018 Faenza, Italy

ARTICLE INFO

ABSTRACT

Engineered Nanomaterials (ENMs) have several uses in various industrial fields and are embedded in a myriad of consumer products. However, there is continued concern over the potential adverse health effects and environmental impacts of ENMs due to their unique physico-chemical characteristics. Currently, there are no specific international regulations for various ENMs. There are also no Occupational Exposure Limits (OEL) regulated by the European Union (EU) for nanomaterials in the form of nano-objects, their aggregates or agglomerates (NOAA). For ENMs the question of which metric to be used (i.e., mass, surface area, number concentrations) to determine the exposure is still not resolved. The aim of this work is to assess the worker exposure by inhalation in an industrial spray coating process by using all three metrics mentioned above. Two target ENMs (N-doped TiO_2, TiO_2N and AgNPs capped with a quaternized hydroxyethyl-cellulose, AgHEC) generated for industrial-scale spraying processes were considered. Results showed that the averaged particle number concentration (10–100 nm) was below $2.7\ 10^4$ cm^{-3} for both materials. The Lung Deposited Surface Area (LDSA) was in the range between 73 and 98 μm^{2}cm^{-3} and the particle mass concentration (obtained by means of ICP-EOS off-line analysis) resulted below 70 μg m^{-3} and 0.4 μg m^{-3} for TiO_2 and Ag, respectively. Although, the airborne particles concentration compared well with the NIOSH Recommended Exposure Level (REL) limits the contribution to the background, according to EN 17058 (Annex E) was significant (particularly in the particle number and PM1 mass concentrations). We successfully evaluated the worker exposure by means of the different airborne particles' metrics (number, surface and mass concentrations). We concluded that worker exposure assessment involving ENMs is a complex procedure with requires both real time and off-line measurements and a deep investigation of the background.

1. Introduction

Engineered Nanomaterials (ENMs) have several uses in various industrial fields and are embedded in a myriad of consumer products such as in cosmetics and personal care products, paints and coatings, food processing and packaging, textiles and clothing, plastics, electronic and optical devices, pesticides, pharmaceutical and medical applications, construction materials, water treatment and environmental remediation etc., either to improve the effectiveness of existing applications or future ones. Consequently, nanotechnology is a fast-growing market that promises to achieve improvements in different areas of life and work. However, there is growing concern over the potential adverse health effects and environmental impacts of ENMs due to their unique physico-chemical characteristics, that account for their widespread industrial

use but, may also be responsible for possible toxic effects (Nel et al., 2006.; Oberdörster et al., 2005). Human exposure to ENMs may occur at any stage of the ENM's lifecycle (from production to use and disposal of consumer products containing ENMs), although it is more likely to occur during the production phase in industrial plants (Iavicoli et al., 2018). Spraying process, a well-known industrial technique consisting of depositing suspensions of various ENMs to coat a variety of different shaped materials, causes high releases of submicron particles (Bekker et al., 2014; Ding et al., 2017; Salmatonidis et al., 2019).

Currently, there are no specific regulations for various ENMs at work. ENMs are subjected to the general regulations for the protection on workers from the risk of chemical agents (Directive 98/24/EC) and to Directive 2004/37/EC in case of carcinogens, mutagens or ENMs toxic to reproduction. Although there are some national initiatives, there are no Occupational Exposure Limits (OEL) regulated by the European Union (EU) for nanomaterials in the form of nano-objects, their aggregates or agglomerates (NOAA). In any event, the NIOSH Recommended Exposure Levels (REL) and Nano Reference Values (NRV) are noteworthy and widely used as substance-specific and categorical OELs respectively for ENMs. A list of proposed OELs for ENMs has been compiled by World Health Organization and is available at WHO, 2017. However, there are general rules and recommendations to protect workers, proposed by several institutions (Oberbek et al., 2019). The assessment of workplace exposure by inhalation of NOAA is standardized, on a voluntary basis, by the EN 17058:2018 EU Standard (EN 17058, 2018), which provides guidance on the sampling and measurement strategies to be adopted and methods for the data evaluation. For ENMs the question of which metric to be used (i.e., mass, surface area, number concentrations) to determine the exposure is still not resolved (Dahmann, 2016) even though, the exposure/dose-response studies shows that mass is a rough indicator for a biologically effective dose for complex occupational aerosols (Kuempel et al., 2014; Braakhuis et al., 2016; Noël et al., 2017; Fadeel et al., 2018).

The aim of this work is twofold:

1) to assess the worker exposure and risk by inhalation in an industrial spray coating process by using all three fundamental metrics: mass, surface area and number concentrations;
2) to correlate an estimation of exposure to each spray coating conditions by using conversion factors between gravimetric particulate matter (PM) assessment on filters and real time measurements by optical particles counters (OPC), that can be associated to each spray tests while PM determination requires longer sampling time.

Measurements were carried out in the framework of the EU Research Project "Anticipating Safety Issues at the design stage of NAno product development" (ASINA, H2020-GA 862444) which aims to support the industrial uptake of nanotechnology by providing Safe by Design (SbD) solutions and supporting tools to broaden the awareness and understanding among stakeholders of the SbD's potential in areas such as functional textiles, air purifying membranes and cosmetics (Furxhi et al., 2021; Furxhi et al., 2022). The ASINA project includes exposure field campaigns to assess the emission of ENMs from lab-scale and industrial-scale spray coating processes in the production of antimicrobical/self-purifying polyester textiles and plastic (polymethyl methacrylate-PMMA) surfaces. Two target ENMs (N-doped TiO$_2$, TiO$_2$N and Ag nanoparticles (NPs) capped with a quaternized hydroxyethyl-cellulose, AgHEC) generated for industrial-scale spraying processes were considered. TiO$_2$ and Ag NPs were identified as target materials because of their industrial scale relevance as antimicrobial/self-purifying additives (Barret et al., 2001; Bickley et al., 1991; Gupta and Silver, 1998; Lee and Park, 2013) for different kinds of products as investigated within the ASINA project.

2. Materials and methods

This work is based on the measurements reported by Del Secco (Del Secco et al., 2022) where the details related to the materials, processes, work environment, instrumentation and concentration measurements are reported. Del Secco et al., (2022) describe the measurements and spray process while Koivisto et al. (2022) describe the exposure scenario concept and process specific emissions factors for worker exposure assessment. In addition, the data are also captured and reported in a Findable, Accessible, Interoperable and Reusable (FAIR) manner (Furxhi et al., 2021). The coating machine, implemented at Wiva Group srl (now Witek srl, Florence, Italy), is a conveyor belt operated, that transfers the substrate through a plasma neutralizer to the spray chamber and then to a drying oven (Fig. 1 above). The machine is designed for coating up to 120 cm wide textile and plastic substrates. The plasma neutralizer is optionally used to remove surface charge from the substrate. Spraying is performed inside a ventilated chamber. Fully automated sprayer consists of four spray nozzles operating with either one, two or four nozzles at the same time. The four nozzles are attached to a mobile element of the machine, that move horizontally on the substrate, always at the same height. The spray nozzle operated with 270 normal L/min air flow atomizing the coating suspension fed at a flow rate of 200 mL/min per nozzle. After spraying, the substrate is dried in the drying oven at low temperature. The spray chamber volume is about 6 m^3 in volume with a clean air inflow rate of about 3000 m^3/h and a bottom aspiration flow to maintain under pressure conditions inside the chamber. The air extracted from the spray chamber is cleaned by a M4 filter before being discharged into the atmosphere. No forced ventilation is present in the working area which is sometimes naturally ventilated by opening windows or doors. The room containing the spray machine is about 6 × 15 m. Since the process is continuous, the cabin cannot be completely sealed on account of the conveyor belt entrance and exit. The coating machine is operated by one worker which divides his time between uploading the panels to be sprayed (sample position, Fig. 1 left), supervising the nozzles and retrieving the coated panels at the oven exit (FF position). The panel uploading position can be considered equivalent to the FF position. Therefore, even if both experimental campaigns should be considered a simulated exercise, we can reasonably assume that the operator spends about 6 h at the FF and 2 h at the Near Field (NF) positions. NF position was near the conveyor belt between the spray chamber and the oven (Fig. 1), and outside the tunnel connecting them. Particles are released from the tunnel to the NF via open holes where worker exposure can occur.

Two NPs suspensions were used at the spray guns: TiO$_2$N (ERM00000560) dispersed in EtOH (1% w/w) and AgHEC (ERM00000559), dispersed in water at concentrations of 0.1%, 0.05% and 0.01% w/w. Specifically, TiO$_2$N suspension was prepared by Colorobbia Italia, SPA (Sovigliana Vinci, FI, Italy) and the AgHEC aqueous nano suspensions was synthetized in CNR-ISSMC (Faenza, Italy) by a patented synthesis process (Costa and Blosi, 2016). The European Registry of Materials (ERM) identifiers ensure that the internal project documentation can later be linked to publicly released data and knowledge for the specific NPs; the full list can be found at https://nanocommons.github.io/identifiers (van Rijn et al., 2022).

Measurements took place in the period 15th–18th of February 2021 (1st campaign) and 8th–11th of November 2021 (2nd campaign).

- On 15th February and 8th November instruments were set-up and background concentration measurements were carried out with real time and offline PM samplers.
- On 16th February, TiO$_2$N were sprayed both on Polymethylmethacrylate (PMMA) panels and polyester textile substrates, while on 17th February AgHEC were sprayed on polyester textile (PE).
- On November 9th, ethanol and TiO$_2$N NPs were sprayed both on PMMA and PE substrates while in the other measurement days
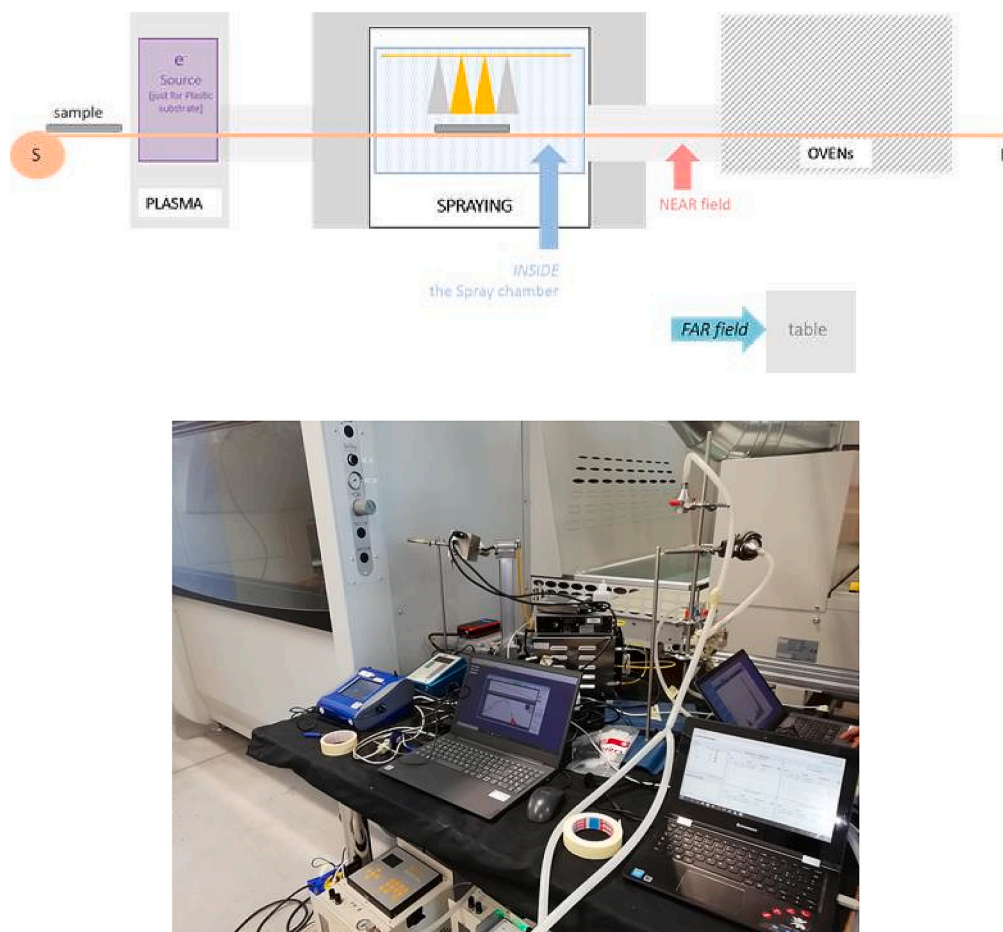
Fig. 1. Above: Schematization of the Witek s.r.l plant and measurement stations (inside, NF and FF). Below: Picture of the sampling station at NF.

(10th–11th November) HEC suspension and AgHEC NPs were sprayed on PE and PMMA supports. Supplementary tests (both TiO$_2$N and AgHEC) were carried out for 15 consecutive minutes (two spray guns) in order to collect data for the mass balance dispersion model used to assess worker exposure concentrations (Koivisto et al., 2022).

- Another additional test was conducted by changing the spray chamber local exhaust flow rate by modifying the power supply percentage to the aspiration pump engine (30% - 80%) compared to normal condition of 55%.

Tables S1 and S2 gives a summary of the tests performed at each experimental campaign. For each kind of suspension, several tests were carried out combining three operational parameters: suspension concentration, flow rate and substrate type (PE and PMMA). Each test, made of 4 sprays, lasted about 40 min.

This study has deployed an area sampling strategy (stationary) to assess occupational inhalation exposure of workers, combining direct reading instruments (DRI) and filter samplers, placed at various fixed locations in the work area and, in particular, near hot spots of concern. During the campaign, measurements were obtained at three different positions: inside the spray chamber, near field (NF) and far field (FF) (Fig. 1). NF position was near the conveyor belt between the spray chamber and the oven, and outside the tunnel connecting them. Particles are released from the tunnel to the NF via open holes where the worker exposure can occur.

In the specific, inside the spray chamber aerosol number concentration was measured by means of a low-cost optical particles counter SPS30 (Sensirion, Staefa, Switzerland). Aerosol mass concentration was detected by means of an aerosol photometer (DustTrack mod. 8520, TSI

Inc., Shoreview, MN, USA) and by sampling the particles on a PTFE filter (1 μm porosity Ø 47 mm). Gravimetric off-line aerosol mass concentration was determined by weighing the filter before and after the deposition (Del Secco et al., 2021). Measurements inside the spray chamber took place for the purpose of obtaining data on material consumption and to verify that both campaigns gave the same order of magnitude of particle concentrations at the same spray conditions.

Outside the spray chamber size resolved particle concentrations and mass concentrations were measured at NF and FF at heights from 1 to 1.3 m. Details of the instrumentation are given in (Del Secco et al., 2022). The real time NF particle measurement position included, among other instruments, two optical particles counters (OPCs) in the size range from 0.25 to 30 μm (in 32 channels) (11-D and 11-A, GRIMM Aerosol Technick, Ainring, Germany) with a time resolution of 6 s. OPCs 11-D and 11-A were positioned at NF and FF, respectively. These OPCs comply with EN 481 for workplace monitoring of inhalable, thoracic, and respirable dust fractions. However, OPCs do not cover the size range of primary nano-objetcs and their smaller aggregates/agglomerates (EN17058:2019, Annex A). Therefore, particle mobility size distributions in the smaller size range (> 10 nm) were obtained, at NF, by a Scanning Mobility Particle Sizer (SMPS), composed by a differential mobility analyzer (L-DMA mod. Grimm mod. 5400, Grimm Aerosol, Ainring, Germany), a condensation particle counter (CPC, Grimm mod. 5403, Grimm Aerosol, Ainring, Germany), and an X-ray soft charges neutralizer (TSI mod. 3088; Shoreview, MN, USA) instead of the original one based on ^{241}Am (Grimm Mod. 5522). Nicosia and colleagues applied a TSI soft X-Ray neutralizer to the Grimm L-DMA column obtaining a transfer function to correct the data (Nicosia et al., 2018). The SMPS scan time was ca 4.5 min with a 1.5 min retrace time.

Lung Deposited Surface Area (LDSA) was measured at NF and FF stations by means of two Partectors (Nanoeos). Off-line gravimetric PM samples (total fraction) were taken simultaneously inside the spray chamber, at NF and at FF stations (at FF station only during the 2nd campaign) by collecting the particles on absolute filters (PTFE, 1 μm porosity) at 50 L/min flow rate (Bravo H-Plus, TCR Tecora, Italy). PM determinations on the filters were obtained by weighing the filters before and after sampling on a five digits analytical balance (Mettler, Toledo AX105). Afterwards, the filters were acid treated by microwaves digestion to obtain the elemental Ti and Ag content. The microwave system EM-45/A Milestone was used to digest the samples which were analysed by an ICP-OES 5100-vertical dual view apparatus (Agilent Technologies, Santa Clara, CA, USA), coupled with OneNeb nebulizer and equipped with an Autosampler.

The NF and FF particle concentrations for the different metrics, obtained during the spray tests, were subtracted from the background concentrations as given as below:

$$X_{ij} = Xm_{ij} - Xb_j \qquad (1)$$

where X_{ij} stands for one of the three used metrics (PM, LDSA and fine particle number concentrations), i is the test number of the j measurement day. Xm_{ij} is the measurement obtained during test i of day j and Xb_j is the background of the measurements' day j.

The standard deviation is obtained by the error propagation formula:

$$\sigma = \sqrt{\sigma_m^2 + \sigma_b^2} \qquad (2)$$

where σ_m and σ_b are the standard deviation of the measurement and the background concentrations, respectively.

3. Results

3.1. Background concentration

Exposure assessment of ENMs faces a specific problem as there is virtually always a quite substantial background concentration of ultrafine particles. Moreover, we should consider the presence of parallel processes and secondary sources, such as the infiltration of the outdoor (atmospheric) aerosol into the warehouse, responsible for the accumulation effect (during lunch time) and for influencing the background concentration. As risk assessment/management only involves those engineered NPs which are handled or synthesized in a company, the need for background discrimination/control in order to prevent ultrafine particles from falsifying the results is high (Koivisto et al., 2011).

In our measurements the background particle number, surface area and mass concentrations were monitored the day before starting the monitoring campaign and each morning before starting the spray coating machine at NF and FF positions. In addition, at the end of the day after the spray tests, background concentrations were monitored to infer any NPs accumulation inside the warehouse. A further background measurement took place in the 1st campaign during lunch time break at NF and FF positions.

Fig. 2 shows the background concentrations in different metrics obtained during the 1st monitoring campaign at FF. We note that:

a) during lunch time the coarse (1 μm to 10 μm in diameter) particle number and mass concentrations decrease due to their settling, while the fine particle fraction (0.25–1 μm in diameter) remains at the same concentration level or increases due to an accumulation effect (the same for the LDSA);

b) the FF position was influenced by the spray coating process as resulted from the comparison between concentrations before (BEFORE) and after (AFTER) the spray tests;

c) the measurements obtained on 15th February (grey bars) cannot be considered representative of the background presents during the spray tests carried out in the following days, when outdoor aerosol concentrations might have been higher and infiltrates into the warehouse as highlighted in the following item;

d) on 17th February (a cloudy day) the background concentration (orange bars) BEFORE was higher than LUNCH for all particle size fractions. After lunch time, on this day, a secondary source of aerosol, from a track exhaust, infiltrated into the warehouse. As a result, the tests carried out in the afternoon were not included in this study.

Therefore, reasonable estimated background concentrations for the 1st campaign may be obtained by considering the measurements carried out on 16th February before starting the spray tests and, on 17th February, the average between the concentration values obtained before and at lunch time.
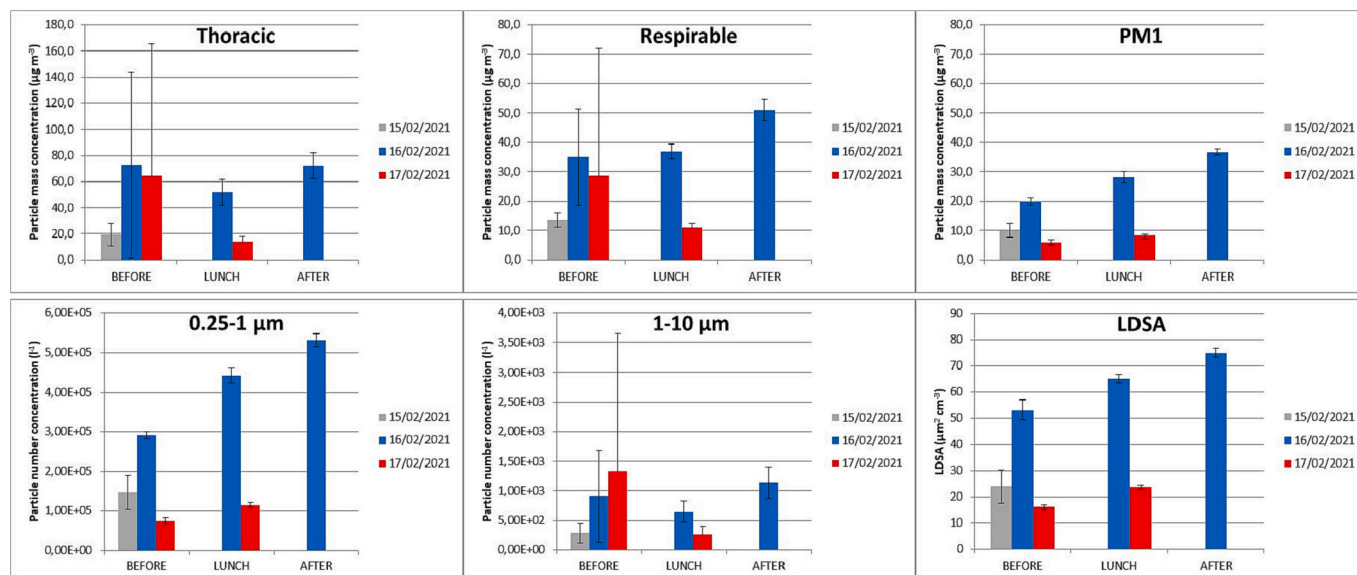

Fig. 2. Background monitoring at FF position during 1st monitoring campaign. Above from left to right: thoracic, respirable and PM1 particle mass fractions measured the day before starting the spray coating operations (15/02/2021), before, during lunch and after the spray coatings the other days. Below from left to right: fine, coarse and LDSA particle number concentrations measured at the same time periods. BEFORE and AFTER mean before and after starting spray coating process, respectively. Bars give one standard deviation. LDSA concentrations were measured by means of a Partector, while other particle concentrations were measured with an OPC-11A.

The same considerations can be extended to the background of the 2nd campaign. Fig. 3 gives FF measurements of health related mass concentration fractions (thoracic and respirable), PM1, LDSA and the particle number concentrations (below and above 1 μm). In general, the concentrations, measured in the spray tests days in the afternoon (after the sprays), were higher than in the mornings. Only on 11th November the LDSA concentration was higher before starting the sprays (both at NF and FF stations). Based on the above considerations, we concluded that the suitable background concentrations were those measured before starting the sprays. Only for LDSA of 11th of November we considered the average between the concentration values before and after. This approach was applied to both NF and FF measurements.

3.2. Spray coating tests: real time results

Results of the 1st and 2nd measuring campaigns are given in Figs. S1-S2 and Figs. S3-S5, respectively. Tables 1 and 2 show the average particle number concentrations (size range 0.25–1 μm), LDSA, the health related averaged mass concentration fractions (thoracic and respirable) and PM1, after background subtraction; in brackets, the average concentrations increased by one standard deviation for the different metrics at NF and FF positions during the 1st and 2nd campaign.

By comparing Table 1 and Table 2 we note that for the same tests the measured aerosol concentrations in the 2nd campaign, at NF position, were lower than during the 1st campaign. Fig. 4 shows the scatter plot of the particle number concentrations measured inside the spray chamber by means of low-cost sensor (SPS30, Sensirion) and by means of an aerosol photometer (DustTrack mod.8520, TSI) for the same tests carried out during the 1st and 2nd campaign. Results show that particle number and mass concentrations, measured inside the spray chamber, were comparable between the two campaigns at the same spray test conditions.

Therefore, in addition to instrument uncertainties, the aerosol concentrations measured at the NF position could be influenced, by the instrument inlet coordinates, which could not be exactly replicate for the two campaigns. In addition, whereas during the 1st campaign the warehouse windows were kept close, in the 2nd campaign they were kept open. This could have changed the environmental ventilation conditions inside the warehouse.

Fig. 5 shows particle number concentrations measured at NF by means of the SMPS in the size range 10–100 nm.

3.3. Spray coating tests: Gravimetric and elemental determinations

Table 3 shows the PM and elemental concentrations (ICP-OES data for Ti were converted in TiO_2 content) obtained from the sampled filters.

The particle mass concentrations, given by OPCs for the same filter sampling time, were compared with the PM gravimetric assessment. Table 4 shows the ratios between the gravimetric PM content and OPCs PM fractions. In addition, also the ratios between the TiO_2 and Ag content and OPCs PM fractions are given. Indeed, data provided by the OPCs must be corrected since the algorithm used to calculate PM fractions (thoracic, respirable and PM1) is not disclosed by the manufacturer (Chakrabarti et al., 2004; Santi et al., 2010; Wu et al., 2022).

The average PM/Respirable fraction ratio for TiO_2N sprays at NF and FF is 2.8 ± 2.1 (ratio values: 1.3–1.9-5.1). In case of AgHEC sprays the same average ratio is 2.8 ± 0.6 (ratio values 3.0–3.5-2.2-2.5). Therefore, on average the ratio PM/Respirable fraction is about 2.8 both for TiO_2 and Ag sprays (even though with higher variability in case of TiO_2 sprays), while for background measurements the ratio is 1.7 (standard deviation 0.2).

4. Discussion

4.1. Exposure assessment

4.1.1. Metric: particle number concentration (fine fraction, < 1 μm)

By considering the OPCs results the worst case scenario, 800 mL/min, (WCS) is given by tests 3 and 6 at 800 mL/min with TiO_2N (Table 1). Substrate PMMA gives an upper level concentration (average plus one standard deviation) of 1.3×10^3 cm^{-3} with an averaged concentration of about 6×10^2 cm^{-3} (test 3). Spraying on PE substrate (test 6) shows little higher concentrations: upper level concentration 1.6×10^3 cm^{-3} with an averaged concentration of about 8×10^2 cm^{-3}. In the 2nd campaign the trend was the same (higher concentration with spraying on PE) but with lower concentration values.

The standard case scenario, 400 mL/min, (SCS), characterized by a 400 mL/min spray flow rate, was carried out only in the 1st campaign and shows comparable particle number concentrations for PMMA and PE substrates. The upper level concentration is between 5 and 7×10^2
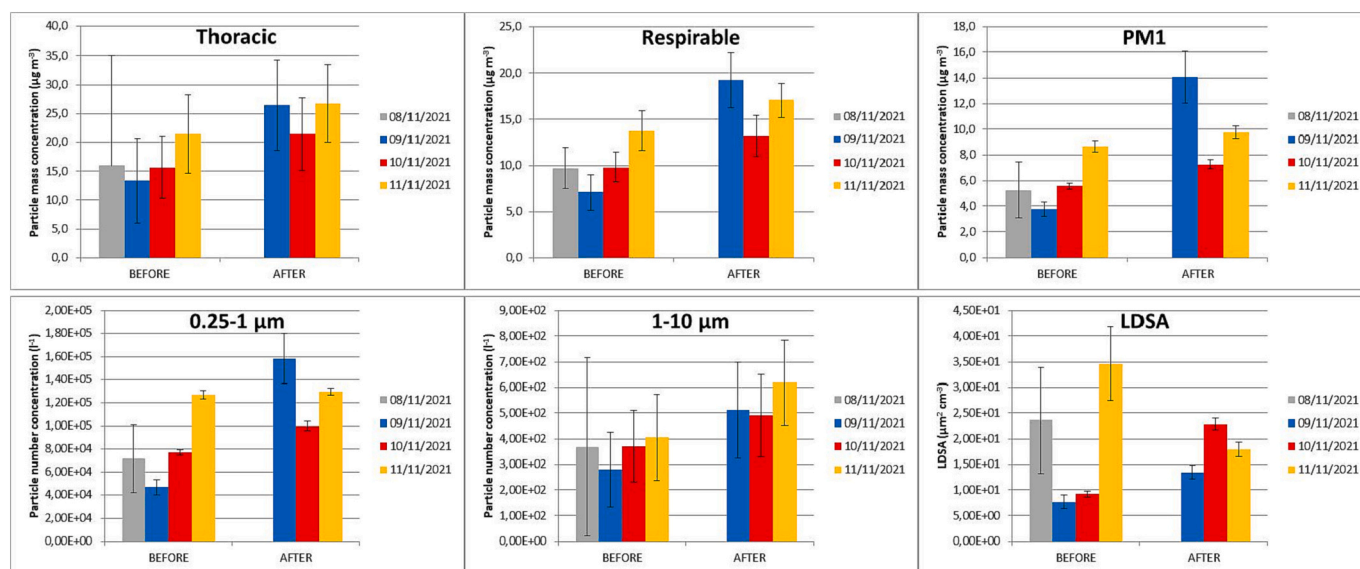

Fig. 3. Background monitoring at FF position during 2nd monitoring campaign. Above from left to right: thoracic, respirable and PM1 particle fractions measured the day before starting the spray coating operations (08/11/2021), before and after the spray coatings the other days. Below from left to right: fine, coarse and LDSA particle number concentrations measured at the same time periods. BEFORE and AFTER mean before and after starting spray coating process, respectively. Bars give one standard deviation. LDSA concentrations were measured by means of a Partector, while other particle concentrations were measured with an OPC-11A.

Table 1

Average PM, LDSA and fine particle number concentrations during the 1st experimental campaign. Tests characteristics are given in the first column. In brackets, the average concentrations increased by one standard deviation. The lowest detectable concentration was imposed in case of negative values after background subtraction: particle number concentration: 1 cm^{-3}; LDSA concentration: 1 µm^2 cm^{-3} and PM fractions: 1 µg m^{-3}. Tests repeated during the 2nd campaign are highlighted in bold characters. LDSA concentrations were measured by means of Partectors, while other particle concentrations were measured with OPC-11A (FF) and OPC-11D (NF).

Test	Particle number conc. (0.25–1) µm (cm^{-3})	LDSA (µm^2 cm^{-3})	Thoracic Fraction (µg m^{-3})	Respirable Fraction (µg m^{-3})	PM1 (µg m^{-3})
1- TiO$_2$N 200 mL PMMA	**NF: 1.4 10^2 (3.3 10^2) FF: 0.6 10^2 (1.2 10^2)**	**NF: 19 (38) FF: 4 (9)**	**NF: 11 (60) FF: 1**	**NF: 19 (53) FF: 1 (19)**	**NF: 14 (35) FF: 4 (8)**
2- TiO$_2$N 400 mL PMMA	NF: 3.5 10^2 (5.4 10^2) FF: 1.9 10^2 (2.2 10^2)	NF: 58 (90) FF: 19 (24)	NF: 72 (135) FF: 17 (90)	NF: 60 (110) FF: 20 (37)	NF: 33 (66) FF: 14 (39)
3- TiO$_2$N 800 mL PMMA	**NF: 5.6 10^2 (1.3 10^3) FF: 2.3 10^2 (2.7 10^2)**	**NF: 73 (179) FF: 21 (60)**	**NF: 126 (349) FF: 11 (84)**	**NF: 113 (305) FF: 22 (40)**	**NF: 60 (145) FF: 19 (63)**
4- TiO$_2$N 200 mL PE	NF: 2.3 10^2 (4.0 10^2) FF: 1.5 10^2 (1.7 10^2)	NF: 33 (50) FF: 10 (16)	NF: 19 (64) FF: 1 (73)	NF: 27 (57) FF: 6 (23)	NF: 21 (40) FF: 10 (11)
5- TiO$_2$N 400 mL PE	NF: 3.7 10^2 (7.0 10^2) FF: 2.2 10^2 (2.4 10^2)	NF: 51 (87) FF: 18 (23)	NF: 66 (166) FF: 1 (78)	NF: 54 (118) FF: 18 (23)	NF: 34 (71) FF: 15 (17)
6- TiO$_2$N 800 mL PE	**NF: 7.8 10^2 (1.6 10^3) FF: 3.1 10^2 (3.6 10^2)**	**NF: 98 (208) FF: 26 (33)**	**NF: 166 (382) FF: 25 (100)**	**NF: 146 (342) FF: 32 (50)**	**NF: 80 (177) FF: 23 (27)**
7- AgHEC (0.01%) 200 mL PE	NF: 0.2 10^1 (3.6 10^1) FF: 0.1 10^1 (1.0 10^1)	NF: 2 (4) FF: 1 (2)	NF: 1 (139) FF: 1 (54)	NF: 1 (74) FF: 1 (24)	NF: 1 (4) FF: 1 (2)
8- AgHEC (0.01%) 400 mL PE	NF: 0.8 10^1 (4.8 10^1) FF: 0.1 10^1 (1.2 10^1)	NF: 22 (29) FF: 15 (21)	NF: 1 (140) FF: 1 (54)	NF: 1 (75) FF: 1 (24)	NF: 1 (4) FF: 1 (2)
9- AgHEC (0.05%) 200 mL PE	**NF: 3.2 10^1 (7.3 10^1) FF: 1.1 10^1 (1.2 10^1)**	**NF: 11 (15) FF: 7 (9)**	**NF: 1 (140) FF: 1 (54)**	**NF: 1 (75) FF: 1 (24)**	**NF: 3 (8) FF: 1 (2)**
10- AgHEC (0.05%) 400 mL PE	NF: 6.6 10^1 (13.7 10^1) FF: 2.1 10^1 (3.0 10^1)	NF: 15 (22) FF: 8 (10)	NF: 1 (141) FF: 1 (53)	NF: 3 (77) FF: 1 (24)	NF: 7 (15) FF: 2 (3)

Table 2

Average PM, LDSA and fine particle number concentrations during the 2nd experimental campaign. Tests characteristics are given in the first column. In brackets, the average concentrations increased by one standard deviation. The lowest detectable concentration was imposed in case of negative values after background subtraction: particle number concentration: 1 cm^{-3}; LDSA concentration: 1 µm^2 cm^{-3} and PM fractions: 1 µg m^{-3}. Common tests between both campaigns are highlighted in bold characters. LDSA concentrations were measured by means of Partectors, while other particle concentrations were measured with OPC-11A (FF) and OPC-11D (NF).

Test	Particle number conc. (0.25–1) µm (cm^{-3})	LDSA (µm^2 cm^{-3})	Thoracic Fraction (µg m^{-3})	Respirable Fraction (µg m^{-3})	PM1 (µg m^{-3})
3- TiO$_2$N 200 mL PMMA	**NF:1.7 10^1 (8.1 10^1) FF:1.4 10^1 (2.6 10^1)**	**NF:14.6 (25.6) FF:3.7 (5.9)**	**NF:7.5 (21.1) FF: 1.0 (10.0)**	**NF:7.7 (17.2) FF: 1.3 (4.0)**	**NF: 5.9 (12.7) FF: 1.3 (2.4)**
4- TiO$_2$N 800 mL PMMA	**NF:2.5 10^2 (6.7 10^2) FF:0.8 10^2 (1.3 10^2)**	**NF:28.2 (53.6) FF: 8.6 (10.3)**	**NF:42.5 (106.0) FF:7.8 (18.8)**	**NF:40.7 (101.7) FF: 8.2 (11.6)**	**NF:3.1 (7.6) FF:7.1 (9.3)**
5- TiO$_2$N 200 mL PE	**NF:1.1 10^2 (1.8 10^2) FF:1.0 10^2 (1.2 10^2)**	**NF:13.8 (20.0) FF:7.9 (10.3)**	**NF:16.7 (31.2) FF:7.7 (16.9)**	**NF:17.0 (27.4) FF:9.3 (12.2)**	**NF:14.7 (22.3) FF:8.9 (10.8)**
6- TiO$_2$N 800 mL PE	**NF:2.8 10^2 (6.5 10^2) FF:1.1 10^2 (1.5 10^2)**	**NF:26.0 (50.0) FF:7.8 (10.2)**	**NF:42.8 (108.6) FF:10.6 (22.8)**	**NF:43.9 (106.3) FF:10.9 (16.2)**	**NF:34.0 (74.5) FF:10.4 (14.2)**
7- HEC (0.1%) 200 mL PMMA	NF:1.0 10^1 (1.5 10^1) FF:0.9 10^1 (9.4 10^1)	NF:52.5 (75.8) FF:32.7 (33.6)	NF:1.9 (20.2) FF:2.1 (20.7)	NF:1.9 (8.7) FF:1.2 (12.3)	NF:1.8 (2.0) FF:1.0 (6.8)
8- HEC (0.1%) 200 mL PE	NF: 1.7 10^1 (2.1 10^1) FF: 1.8 10^1 (2.1 10^1)	NF: 6.7 (8.8) FF: 6.4 (7.4)	NF:0.3 (16.3) FF:0.2 (7.5)	NF:1.3 (6.4) FF:1.2 (3.4)	NF:1.2 (1.8) FF:1.2 (1.6)
10- HEC (0.05%) 200 mL PE	NF: 0.7 10^1 (1.3 10^1) FF: 0.6 10^1 (0.9 10^1)	NF:1.8 (4.6) FF: 1.3 (2.3)	NF:1.0 (17.1) FF:1.0 (8.5)	NF:1.0 (5.5) FF:1.0 (2.0)	NF:1.0 (2.0) FF:1.0 (2.0)
11- HEC (0.05%) 400 mL PE	NF: 1.0 10^1 (1.8 10^1) FF: 0.9 10^1 (1.4 10^1)	NF: 3.8 (6.6) FF: 3.9 (5.1)	NF:1.0 (17.2) FF:1.0 (8.4)	NF:1.0 (6.2) FF:1.0 (3.2)	NF:1.0 (2.1) FF:1.0 (2.0)
12- AgHEC (0.05%) 200 mL PE	**NF: 1.3 10^1 (2.1 10^1) FF: 0.8 10^1 (0.8 10^1)**	**NF: 2.5 (4.8) FF: 2.5 (2.0)**	**NF:1.0 (17.1) FF:1.0 (11.1)**	**NF:1.0 (1.5) FF:1.3 (4.1)**	**NF:1.0 (2.0) FF:1.0 (2.0)**
13- AgHEC (0.05%) 400 mL PE	**NF: 1.8 10^1 (2.6 10^1) FF: 0.9 10^1 (1.3 10^1)**	**NF: 4.4 (6.9) FF: 2.1 (3.0)**	**NF: 1.0 (2.7) FF: 1.0 (2.0)**	**NF: 1.0 (6.0) FF: 1.0 (3.6)**	**NF: 1.4 (2.4) FF: 1.0 (2.0)**
14- AgHEC (0.05%) 200 mL PMMA	NF: 1.9 10^1 (3.0 10^1) FF: 1.1 10^1 (1.5 10^1)	NF: 5.3 (7.5) FF: 3.2 (3.5)	NF: 1.0 (16.7) FF: 1.0 (8.9)	NF: 1.0 (6.1) FF: 1.0 (3.3)	NF: 1.5 (2.5) FF: 1.0 (2.0)
15- AgHEC (0.05%) 400 mL PMMA	NF: 2.5 10^1 (3.4 10^1) FF: 2.0 10^1 (2.7 10^1)	NF:10.5 (13.4) FF:10.4 (13.2)	NF: 1.0 (17.2) FF: 3.1 (10.9)	NF: 1.9 (7.0) FF: 2.2 (4.6)	NF: 1.9 (2.9) FF: 1.4 (2.4)
16- AgHEC (0.1%) 200 mL PE	NF: 1.8 10^1 (4.6 10^1) FF: 0.7 10^1 (1.3 10^1)	NF: 6.0 (9.6) FF: 6.0 (10.5)	NF: 2.6 (13.3) FF: 1.0 (9.6)	NF:3.3 (9.2) FF:1.0 (3.9)	NF:2.2 (5.6) FF:1.0 (2.0)
17- AgHEC (0.1%) 400 mL PE	NF: 1.6 10^1 (3.6 10^1) FF: 1.7 10^1 (3.1 10^1)	NF: 2.3 (6.0) FF: 2.7 (7.6)	NF: 1.0 (10.4) FF: 1.0 (9.8)	NF: 2.0 (6.6) FF: 1.0 (4.1)	NF: 1.9 (4.3) FF: 1.5 (2.7)
18- AgHEC (0.1%) 200 mL PMMA	NF:1.5 10^1 (3.4 10^1) FF:1.1 10^1 (1.7 10^1)	NF: 5.0 (8.9) FF: 4.1 (8.8)	NF: 1.2 (10.6) FF: 1.0 (11.1)	NF: 2.0 (5.8) FF: 1.0 (4.0)	NF: 1.6 (3.0) FF: 1.0 (2.0)

cm^{-3} with an averaged concentration of about 4 10^2 cm^{-3}. These concentration values, background subtracted, are considered as composed by TiO$_2$N particles (being on the safe side).

The WCS for AgHEC sprays is given by tests 17 and 19 (2nd campaign) at 400 mL/min (Ag concentration suspension of 0.1%) on PE and PMMA, respectively. Both substrates give comparable particle number concentrations with an upper concentration level below 4 10^1 cm^{-3} and averaged concentration below 2 10^1 cm^{-3}. These concentration values, even if background subtracted, also contain HEC particles as can be observed from tests 6–11. However, being on the safe side these concentrations will be treated as Ag particles. The Institute for Occupational Safety and Health of the German Social Accident Insurance (IFA 2009) recommended a benchmark limit to be used for an 8-h work shift and to be used for monitoring the effectiveness of protective measures in the workplace of 4 10^4 cm^{-3} in the measured range between 1 and 100 nm (for biopersistent granular nanomaterials with a density below 6 10^3 kg/m^3) (Schulte et al., 2010). Measured averaged, upper level concentrations, after subtraction of the background, did not exceed both

Table 2 (*continued*)

Test	Particle number conc. (0.25–1) μm (cm^{-3})	LDSA (μm^2 cm^{-3})	Thoracic Fraction (μg m^{-3})	Respirable Fraction (μg m^{-3})	PM1 (μg m^{-3})
19- AgHEC (0.1%) 400 mL PMMA	NF: 1.7 10^1 (3.2 10^1) FF: 1.1 10^1 (2.2 10^1)	NF:2.2 (5.7) FF:1.0 (5.9)	NF: 1.0 (10.5) FF: 1.0 (9.7)	NF: 2.2 (6.4) FF: 1.0 (4.0)	NF: 1.8 (3.6) FF: 1.1 (2.2)

recommended benchmarks (see Fig. 5).

4.1.2. Metric: particle surface concentration (LDSA)

Even though LDSA requires further development to enable it as a reliable dose metric because of differences due to particle material and morphology, (Levin et al., 2016) it was still deployed in several exposure studies (Asbach et al., 2017). WCS is also given for tests 3 and 6 (1st campaign) with averaged values of about 73 and 98 μm^{2}cm^{-3}, respectively. Upper levels were respectively 179 μm^2 cm^{-3} and 208 μm^2 cm^{-3}. In the 2nd campaign the same tests give an LDSA average concentration below 50 μm^{2}cm^{-3} and about 50 μm^{2}cm^{-3} (upper level). The SCS case (400 mL/min) shows an averaged LDSA concentration around 60 μm^{2}cm^{-3} and an upper level concentration of about 90 μm^{2}cm^{-3}. Spray tests using AgHEC recorded lower LDSA values. In general, few reports and literature works reported exposure information, including LDSA

concentrations, thus having a limited availability of these data. However, Geiss et al.(Geiss et al., 2016) gave a review of LDSA concentrations in different occupational and non-occupational environments. In occupational environment LDSA values ranged between 761 and 24.7 μm^2 cm^{-3} (average 137 μm^{2}cm^{-3}) for welding operations, 3927–15 μm^{2}cm^{-3} (average 415 μm^{2}cm^{-3}) canteen kitchen and 277.4–26.4 μm^{2}cm^{-3} (average 77.2 μm^{2}cm^{-3}) car journey. The WCS showed an LDSA concentration comparable with averaged LDSA value in a car journey. Ortelli et al. (Ortelli et al., 2020) in a spray coating process with TiO$_2$ particles measured LDSA concentrations between 138 and 291 μm^{2}cm^{-3} depending on the spray nozzle pressure from 1.5 bar to 4.0 bar and below than 70 μm^{2}cm^{-3} in Ag spray coating process at lab-scale (Trabucco et al., 2021).

LDSA cited measurements were obtained with instruments based on the same principle (diffusion charging). Since no standard calibration procedure has been established so far, measurements carried out by instruments from different manufacturers can differ by 10–30% (Asbach et al., 2017). Thus, the measurement results are directly comparable.

Schmid and Stoeger (Schmid and Stoeger, 2016) evaluated the total particle BET surface area (cm^2) instilled in rats and mice lungs correlation with polymorphonuclear neutrophilia (PMN) for low solubility and low toxicity particles as well as some transition metal oxides. PMN is a strong indicator for lung inflammation and forming acute phase response protein that cause plaque formation in the blood vessels (Saber et al., 2014; Thompson et al., 2018). The relation of surface area dose and PMN influx can be used as an indication of workers risk suffering pulmonary inflammation during an 8-h exposure (Koivisto et al., 2017).
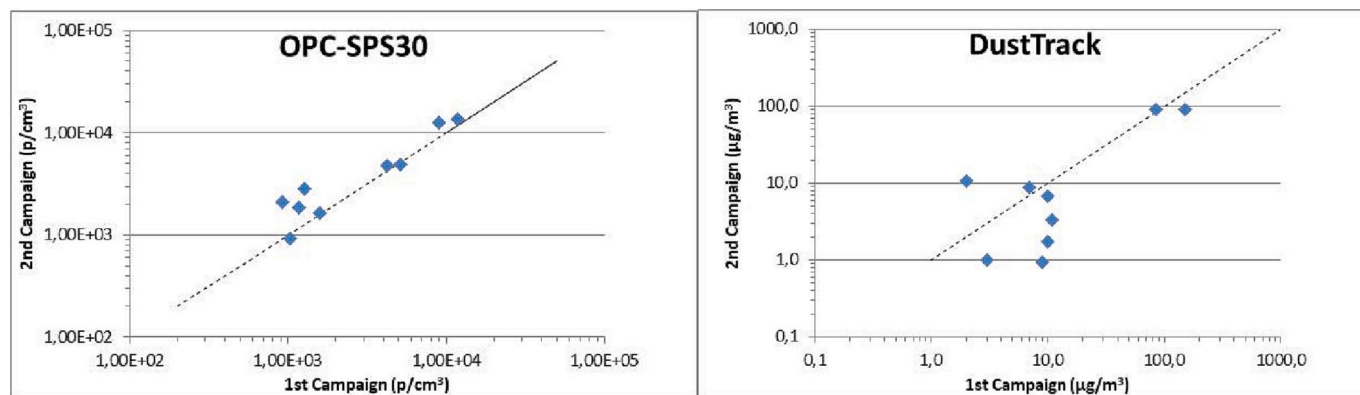

Fig. 4. Particle number and mass concentrations measured inside the spray chamber for the same tests of both experimental campaigns. Left: scatter plot for the particle number concentrations measured by means of the low-cost OPC sensor. Right: particle mass concentration measured by means of the aerosol photometer.
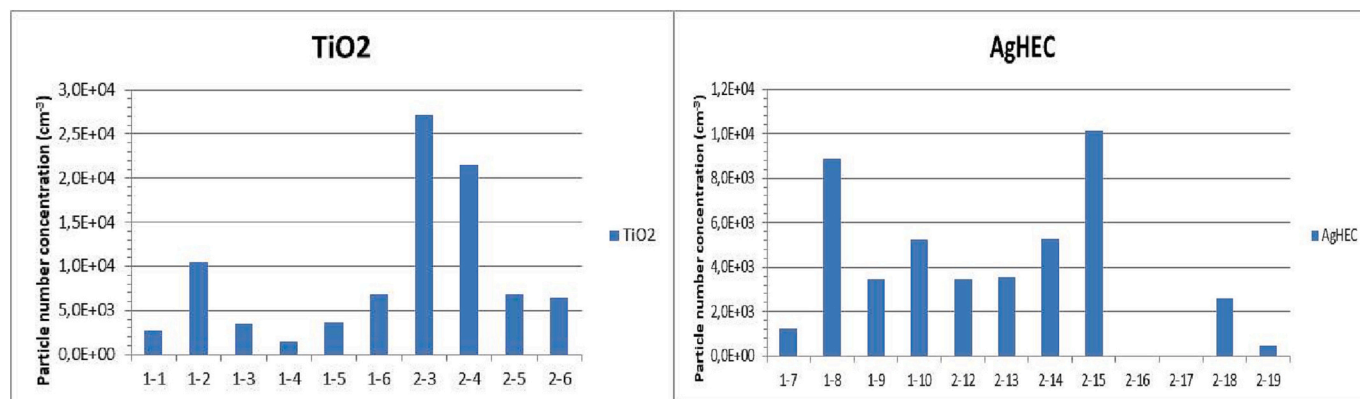
Fig. 5. Particle number concentrations in the size range 10–100 nm. Right: Spray tests carried out with TiO$_2$ suspension; left: spray tests carried out with Ag suspensions. Results are given for both campaigns (1–1 means test 1 of the 1st campaign, 2–3 means test 3 of the 2nd campaign and so on). Particle concentrations were measured with an SMPS. X-axis reports experimental test acronyms; 1–1 means 1st campaign test 1, 1–2 1st campaign test 2, 2–3 2nd campaign test 3, and so forth.

Table 3

PM gravimetric and elemental analysis obtained from the filters sampled during both campaigns at NF and FF (bold characters) positions.

Sampling day and positions	PM Gravimetric ($\mu g\ m^{-3}$)	TiO_2 concentrations ($\mu g\ m^{-3}$)	Ag concentrations ($\mu g\ m^{-3}$)
15/02/2021 Background NF	28 ± 3	0.30 ± 0.03	<0.02
16/02/2021 Test 1–6 NF	120 ± 2	40.92 ± 0.03	<0.02
17/02/2021 Tests 7–13 NF	64 ± 2	<0.03	0.30 ± 0.02
08/11/2021 Background NF	17 ± 1	1.52 ± 0.03	<0.02
08/11/2021 Background FF	**18 ± 1**	**<0.03**	**<0.02**
09/11/2021 Tests 3-TC15_1 NF	76 ± 3	68.73 ± 0.03	<0.02
09/11/2021 Tests 3-TC15_1 FF	**36 ± 2**	**18.80 ± 0.03**	**<0.02**
10/11/2021 Tests 7–11 NF	22 ± 3	<0.03	<0.02
10/11/2021 Test 12–15 NF	42 ± 4	<0.03	<0.12 ± 0.02
10/11/2021 Test 12–15 FF	**24 ± 3**	**<0.03**	**<0.06 ± 0.02**
11/11/2021 Tests 16-TC_15_2 NF		<0.03	0.43 ± 0.02
11/11/2021 Tests 16-TC_15_2 FF	**38 ± 3**		**0.12 ± 0.02**

Table 4

Ratio between PM gravimetric and OPCs particle mass fractions. The two last columns: ratio between ICP-OES elemental analysis results (TiO_2 and Ag) and respirable particle mass fraction obtained from the OPCs.

Sampling day and positions	PM/Thoracic fraction	PM/Respirable fraction	PM/PM1	TiO_2/Resp	Ag/Resp
15/02/2021 Background NF	1.4	1.9	2.8		
16/02/2021 Test 1–6 NF	0.9	1.3	2.2	0.4	
17/02/2021 Tests 7–13 NF	2.1	3.0	5.8		0.02
08/11/2021 Background NF	1.0	1.5	4.3		
08/11/2021 Background FF	1.1	1.8	3.6		
09/11/2021 Tests 3-TC15_1 NF	1.6	1.9	3.5	1.8	
09/11/2021 Tests 3-TC15_1 FF	2.8	5.1	9.0	2.7	
10/11/2021 Tests 7–11 NF	1.2	2.0	4.4		
10/11/2021 Tests 7–11 FF					
10/11/2021 Test 12–15 NF	2.5	3.5	7.0		0.01
10/11/2021 Test 12–15 FF	1.4	2.2	4.0		0.00
11/11/2021 Tests 16-TC_15_2 NF					0.03
11/11/2021 Tests 16-TC_15_2 FF	1.7	2.5	3.8		0.01

They estimated workers' risk for suffering acute pulmonary inflammation by comparing the human equivalent LDSA 8-h with one hundredth of the no observed effect level (no inflammation) (NOEL$_{1/100}$) derived from (Schmid and Stoeger, 2016). The lung-weight normalized NOEL$_{1/100}$ was 0.11 cm^2 g^{-1} for granular biodurable particles, such as TiO_2. Here, the upper level of LDSA concentration was 208 $\mu m^2 cm^{-3}$. In 8-h exposure duration, this would correspond to the human equivalent dose of 0.03 cm^2 g^{-1} (see calculation details from (Koivisto et al., 2017), which is well below the NOEL$_{1/100}$ for granular biodurable particles.

For transition metal oxides (Co, Ni, and Zn-oxide), the NOEL$_{1/100}$ was 9 10^{-3} cm^2 g^{-1}. The upper level of LDSA concentration was 22 $\mu m^2 cm^{-3}$. In 8-h exposure duration, this would correspond to the human equivalent dose of 0.003 cm^{2}g^{-1}, which is well below the NOEL$_{1/100}$ for transition metal oxides. The first order risk assessment shows that workers suffering inflammatory effects is not relevant.

4.1.3. Metric: particle mass concentration

NIOSH recommends airborne exposure limits (REL) of 2.4 mg/m^3 for fine TiO_2 and 0.3 mg/m^3 for ultrafine (including engineered nanoscale) TiO_2, as time-weighted average (TWA) concentrations for up to 10 h/day during a 40-h work week. These recommendations represent levels that over a working lifetime are estimated to reduce risks of lung cancer to below 1 in 1000. The recommendations are based on using chronic inhalation studies in rats to predict lung tumour risks in humans (NIOSH, 2011). From Table 3 the highest TiO_2 concentration is below 70 $\mu g\ m^{-3}$ obtained during the 2nd campaign. Assuming that work is continuous, based on the NIOSH REL level, lifetime exposure may be considered adequately controlled. The conditions of use for the spray process are specified by Koivisto et al. (2022). It is necessary to underline that one of the tests was done with low ventilation flow rate and therefore the TiO_2 concentration must be considered representative of an inadequate spray chamber ventilation rate. In normal conditions the TiO_2 concentration measured was below 41 $\mu g\ m^{-3}$. By considering the correction factors between PM and respirable fraction and then between respirable fraction and TiO_2 concentration it is possible to estimate the contribution of each test to the TiO_2 concentration levels. Table 5 gives estimated TiO_2 concentrations for the three different cases: 200 mL/min, 400 mL/min (SCS) and 800 mL/min (WCS). The conversion factors were taken from Table 4. Only in the WCS the upper limit of the estimated TiO_2 concentration is higher than the REL value of 300 $\mu g\ m^{-3}$.

Considering a work shift made of 6 h at FF exposure concentrations (panel uploading and off) and 2 h in front of the spray chamber (NF exposure levels) the 8-h weighted exposure to respirable concentrations would be about 62 $\mu g\ m^{-3}$ and 0.4 $\mu g\ m^{-3}$, respectively for TiO_2N and AgHEC spray coatings. These values were obtained by taking into account the bracket values in Table 1 (Respirable fraction column, SCS).

NIOSH recommended exposure limit (REL) of 10 $\mu g\ m^{-3}$ as an 8-h (TWA) concentration (total mass sample) of silver (metal dust, fume, and soluble compounds, as Ag) and 0.9 $\mu g\ m^{-3}$ for particles <100 nm

Table 5

Estimated particle mass concentration (respirable fraction) by means of the OPC at NF station at the 1st campaign. Column two: tests 1, 2 and 6 (from Table 3). Column three: measured concentrations converted into equivalent gravimetric concentrations. Column four: equivalent gravimetric respirable fraction converted into TiO_2 estimated concentrations. In brackets the upper limit concentration: average increased by one standard deviation.

Spray test	OPC Respirable PM concentration ($\mu g\ m^{-3}$)	Equivalent gravimetric respirable fraction 2.8 * OPC Respirable PM concentration ($\mu g\ m^{-3}$)	TiO_2 estimated concentration 0.4 * ($\mu g\ m^{-3}$)
200 mL/min	19 (53)	53 (148,4)	21 (59)
400 mL/min (SCS)	60 (110)	168 (308)	67 (123)
800 mL/min (WCS)	146 (342)	409 (958)	164 (383)

(NIOSH, 2021; Bergeson and Hutton, 2021). From Table 3 the measured Ag concentrations in the total PM were between 0.3 and 0.4 µg m^{-3}. The same estimation exercise carried out with TiO$_2$N sprays could be applied to AgHEC sprays (Table 6). Even in the sprays with higher Respirable fraction OPC measured concentrations (Test 9 and 10, 1st campaign) the estimated upper Ag concentrations at NF would be below the REL limit.

To determine if the exposure to NOAA is significant, the decision rule according to following relationship shall be used according to Annex E in standardized guidelines EN17058 (EN 17058:2018). The application of this decision rule can include all metrics used in this work (Eq. 3).

$$X_{ij} < X_j + 3^*\sigma_j \qquad (3)$$

where X_{ij} is the mean concentration (particle number, surface or mass) of airborne particles during activity, X_j is the background concentration and σ_j is the background standard deviation. If the above relationship is not verified there is a likelihood of exposure induced by NM-activity to the environmental airborne particles' concentration.

Table 7 gives the average background concentrations, already increased with three standard deviations, for each measuring days. The decision rule does not make difference between materials. Therefore, we apply it by considering the SCS and WCS in each sampling day (Table 8, in brackets WCS). Bold characters in Table 8 refer to tests which do not comply with the decision rule.

Although, the airborne particle concentration, once the background was subtracted, compared well with the REL limits in each considered metrics (particle number, surface and mass concentrations) in most WCS tests the contribution to the background was statistically significant (particularly in the particle number and PM1 mass concentrations). This contribution can be observed also at the FF station suggesting a diffusion in the working environment of sprayed particles. However, it should also be considered that real time monitoring does not allow to distinguish between particle composition. Therefore, the elemental content (Ti or Ag concentrations in our study) is a basic information which need to be considered in the monitoring activities. In addition, toxicologically relevant metric is mass because it is the most common metric in dose/exposure response studies. Such studies are scarce for particle number or surface area. However, instruments measuring surface area or particle number concentrations are typically highly sensitive for NP emissions (Koivisto et al. 2019). Thus, they are useful to identify exposure but mass is usually needed for risk characterization. Koivisto et al. (2022) present process-specific emission factors, one of whose variable is suspension Ag-HEC mass concentration. This can be used with reasonable accuracy to model the effect on NF and FF exposure levels.

5. Conclusions

In this work we investigated worker inhalation exposure assessment

Table 6
Measured particle mass concentration (respirable fraction) by means of the OPC at NF station at the 1st campaign. Column two: tests 9 and 10 (from Table 3). Column three: measured concentrations converted into equivalent gravimetric concentrations. Column four: equivalent gravimetric respirable fraction converted into Ag estimated concentrations. In brackets the upper limit concentration: average increased by one standard deviation.

Spray test	OPC Respirable PM concentration (µg m^{-3})	Equivalent gravimetric respirable fraction 2.8 * OPC Respirable PM concentration (µg m^{-3})	Ag estimated concentration 0.03 * (µg m^{-3})
200 mL/min (Ag 0.05%)	1 (75)	3 (210)	0.1 (6)
400 mL/min (Ag 0.05%)	3 (77)	8 (216)	0.2 (6)

Table 7
Averaged airborne particle concentration increased by three times the standard deviation, considering background day indicated in the first column. LDSA concentrations were measured by means of a Partector, while other particle concentrations were measured with an OPC-11A.

Day	Particle number concentration (0.25–1) µm (cm^{-3})	LDSA (µm^2 cm^{-3})	Thoracic Fraction (µg m^{-3})	Respirable Fraction (µg m^{-3})	PM1 (µg m^{-3})
15/02/2021	NF: 2.8 10^2 FF: 2.6 10^2	NF: 58 FF: 43	NF: 48 FF: 46	NF: 31 FF: 26	NF: 18 FF: 17
16/02/2021	NF: 3.0 10^2 FF: 3.2 10^2	NF: 128 FF: 66	NF: 163 FF: 287	NF: 69 FF: 84	NF: 22 FF: 22
17/02/2021	NF: 9.3 10^1 FF: 1.2 10^2	NF: 31 FF: 19	NF: 454 FF: 197	NF: 243 FF: 87	NF: 9 FF: 9
08/11/2021	NF: 1.1 10^2 FF: 1.6 10^2	NF: 52 FF: 55	NF: 53 FF: 73	NF: 28 FF: 28	NF: 8 FF: 12
09/11/2021	NF: 1.2 10^2 FF: 6.7 10^1	NF: 55 FF: 17	NF: 37 FF: 35	NF: 15 FF: 13	NF: 4 FF: 5
10/11/2021	NF: 7.6 10^1 FF: 8.4 10^1	NF: 20 FF: 15	NF: 61 FF: 32	NF: 24 FF: 15	NF: 6 FF: 6
11/11/2021	NF: 1.1 10^2 FF: 1.4 10^2	NF: 44 FF: 36	NF: 40 FF: 42	NF: 20 FF: 20	NF: 8 FF: 10

Table 8
Averaged airborne particle concentrations, considering SCS and WCS (in brackets). Bold characters refer to tests which do not comply with the rule i.e. a significative contribution of the working activity is expected. LDSA concentrations were measured by means of a Partector, while other particle concentrations were measured with an OPC-11D.

Day	Particle number concentration (0.15–1) µm (cm^{-3})	LDSA (µm^2 cm^{-3})	Thoracic Fraction (µg m^{-3})	Respirable Fraction (µg m^{-3})	PM1 (µg m^{-3})
16/02/2021 Test 5 (Test 6)	**NF: 6.3 10^2 (1.0 10^3)** **FF: 5.1 10^2 (6.0 10^2)**	NF: 104 **(151)** FF: **71 (79)**	NF: 124 **(224)** FF: 72 (98)	NF: **87 (179)** FF: 49 (67)	**NF: 53 (99)** **FF: 34 (43)**
17/02/2021 Test 9 (Test 10)	**NF: 1.1 10^2 (1.5 10^2)** FF: 1.1 10^2 **(1.2 10^2)**	NF: 29 **(32)** FF: **23 (24)**	NF: 30 (37) FF: 24 (26)	NF: 19 (25) FF: 14 (16)	**NF: 9 (12)** FF: 8 **(9)**
09/11/2021 Test 5 (Test 6)	**NF: 1.8 10^2 (3.6 10^2)** **FF: 1.4 10^2 (1.6 10^2)**	NF: 23 (35) FF: 16 (16)	NF: 29 **(55)** FF: 21 (24)	NF: **24 (51)** FF: **16 (28)**	**NF: 18 (37)** **FF: 13 (14)**
10/11/2021 Test 12 (Test 15)	**NF: 7.7 10^1 (8.9 10^1)** FF: 8.1 10^1 **(9.7 10^1)**	NF: 13 **(21)** FF: 10 **(20)**	NF: 19 (18) FF: 18 (19)	NF: 13 (12) FF: 11 (12)	NF: 5 **(6)** **FF: 6 (7)**
11/11/2021 Test 18 (Test 19)	**NF: 1.2 10^2 (1.2 10^2)** **FF: 1.4 10^2 (1.4 10^2)**	NF: 36 **(33)** FF: 30 **(26)**	NF: 20 **(20)** FF: 22 **(20)**	NF: 15 (15) FF: 15 (14)	**NF: 8 (9)** **FF: 10 (10)**

by means of the different airborne particles' metrics (number, surface and mass concentrations) and risk based on number concentration benchmark values, deposited surface area response for acute pulmonary inflammation and mass concentration recommended exposure limit (REL) values. The study was based on the results from two field monitoring campaigns carried out in an industrial spray coating plant. Background concentrations were mostly influenced by the aerosol infiltration from outside the warehouse where the spray tests took place.

These were subtracted from concentrations to assess process particle concentration levels in number, surface and mass in NF and FF positions. Spray tests were carried out with different spray flow rate, coating substrates, and spray suspension concentrations to cover different working conditions. The ratio between the OPCs PM fractions (Thoracic, Respirable and PM1) and the gravimetric measurements was used to estimate the equivalent gravimetric PM concentrations in each spray tests. Spray tests with lowest particle emission and acceptable coating effectiveness will be considered in the optimization of the process in the light of Safe-by-Design approach.

Ultrafine particle emissions from spraying process were investigated by conducting blank spray experiments by using the solvent without NPs (ethanol for TiO_2-N and HEC dissolved in water for AgHEC).

In majority of the spray coating tests the process particle concentrations increased significantly in the NF based on the EN17058:2018 decision rule. However, particle number concentrations during spraying of HEC dissolved in water was comparable with AgHEC sprayings. Process particle concentrations in the NF were below the benchmark limit value for number concentration, derived no effect limit for pulmonary inflammation for lung deposited surface area and RELs given for exposure to nano-Ti and Ag mass concentrations. This confirm that the conditions of use as specified by Koivisto et al. (2022) for mass concentrations apply for number and surface area concentrations as well.

Our results highlighted that in case of unsteady emission processes of engineered NPs, made of different materials with different toxicity levels, occupational exposure assessment cannot be based solely on real time measurements without elemental analysis. Our approach compares results from real time measurements with off-line elemental concentrations giving rise to an estimation of the Ag concentration values with an increased time resolution.

In conclusion, worker exposure assessment involving ENMs is a complex procedure with requires both real time and off-line measurements and a deep investigation of the background. The evaluation of worker exposure by means of number, surface and mass concentrations and assessment of concentrations separately from external atmospheric conditions, experimental conditions and suspension characteristics by using blank spray tests is a step forward in the source specific and multimetric exposure assessment.

Franco Belosi (F.B.), Antti Joonas Koivisto (A.J.K.), Irini Furxhi (I.F.), Jesús Lopez de Ipiña (J.L.I.), Alessia Nicosia (A.N.), Fabrizio Ravegnani (F.R.), Simona Ortelli (S.O.), Ilaria Zanoni (I.Z.) and Anna Luisa Costa (A.C.)

Author contributions

Conceptualization, F.B., A.J.K., J.L.I., A.C.; Methodology, F.B., A.J. K., J.L.I.; Investigation, F.B., A.J.K., J.L.I., F.R., I.Z.; Data Curation, F.B., A.J.K., I.F., J.L.I., F.R.; Writing—Original Draft Preparation, F.B.; Writing—Review and Editing, F.B., A.J.K., I.F., A.N., S.O.; Supervision, F.B., A.C.; Funding Acquisition, A.C.

Declaration of Competing Interest

The authors declare that they have no known competing financial interests or personal relationships that could have appeared to influence the work reported in this paper.

Data availability

Data will be made available on request.

Acknowledgments

References

Asbach, C., Alexander, C., Clavaguera, S., Dahmann, D., Dozol, H., Faure, B., Fierz, M., Fontana, L., Iavicoli, I., Kaminski, H., MacCalman, L., Meyer-Plath, A., Simonow, B., van Tongeren, M., Todea, A.M., 2017. Review of measurement techniques and methods for assessing personal exposure to airborne nanomaterials in workplaces. Sci. Total Environ. 603–604, 793–806. https://doi.org/10.1016/J. SCITOTENV.2017.03.049.

Barret, M.C., Mahon, M.F., Molloy, K.C., Steed, J.W., Wright, P., 2001. Synthesis and structural characterization of Tin(II) and Zinc(II) derivatives of cyclic r-hydroxyketones, including the structures of Sn(maltol) 2, Sn(tropolone) 2, Zn (tropolone) 2, and Zn(hinokitiol) 2. Inorg. Chem. 40, 4384–4388. https://doi.org/10.1021/ic0100368.

Bekker, C., Brouwer, D.H., van Duuren-Stuurman, B., Tuinman, I.L., Tromp, P., Fransman, W., 2014. Airborne manufactured nano-objects released from commercially available spray products: temporal and spatial influences. J Expo Sci Environ Epidemiol 24, 74–81. https://doi.org/10.1038/JES.2013.36.

Bergeson, L.L., Hutton, C.N., 2021. NIOSH CIB on Health Effect of Occupational Exposure to Silver Nanomaterials Includes REL for Silver Nanomaterials. https://nanotech.lawbc.com/2021/05/niosh-cib-on-health-effect-of-occupational-exposure-to-silver-nanomaterials-includes-rel-for-silver-nanomaterials/.

Bickley, R.I., Gonzalez-Carreno, T., Lees, J.S., Palmisano, L., Tilley, R.J.D., 1991. A structural investigation of titanium dioxide photocatalysts. J. Solid State Chem. 92, 178–190. https://doi.org/10.1016/0022-4596(91)90255-G.

Braakhuis, H.M., Cassee, F.R., Fokkens, P.H.B., de La Fonteyne, L.J.J., Oomen, A.G., Krystek, P., de Jong, W.H., van Loveren, H., Park, M.V.D.Z., 2016. Identification of the appropriate dose metric for pulmonary inflammation of silver nanoparticles in an inhalation toxicity study. Nanotoxicology 10, 63–73. https://doi.org/10.3109/17435390.2015.1012184.

Chakrabarti, B., Fine, P.M., Delfino, R., Sioutas, C., 2004. Performance evaluation of the active-flow personal DataRAM PM2.5 mass monitor (Thermo Anderson pDR-1200) designed for continuous personal exposure measurements. Atmos. Environ. 38, 3329–3340. https://doi.org/10.1016/J.ATMOSENV.2004.03.007.

Costa, A.L., Blosi, M., 2016. Process for the preparation of nanoparticles of Noble metals in hydrogel and nanoparticles thus obtained. WIPO Patent (WO2016125070A1).

Dahmann, D., 2016. Exposure assessment: methods. In: Handbook of Environmental Chemistry, 48, pp. 51–72. https://doi.org/10.1007/698_2015_436.

Del Secco, B., Trabucco, S., Ravegnani, F., Koivisto, A.J., Zanoni, I., Blosi, M., Ortelli, S., Altin, M., Bartolini, G., Costa, A.L., Belosi, F., 2022. Particles emission from an industrial spray coating process using Nano-materials. Nanomaterials 12, 313. https://doi.org/10.3390/nano12030313.

Ding, Y., Kuhlbusch, T.A.J., van Tongeren, M., Jiménez, A.S., Tuinman, I., Chen, R., Alvarez, I.L., Mikolajczyk, U., Nickel, C., Meyer, J., Kaminski, H., Wohlleben, W., Stahlmecke, B., Clavaguera, S., Riediker, M., 2017. Airborne engineered nanomaterials in the workplace-a review of release and worker exposure during nanomaterial production and handling processes. J. Hazard. Mater. 322, 17–28. https://doi.org/10.1016/J.JHAZMAT.2016.04.075.

EN 17058, 2018. Workplace Exposure - Assessment of Exposure by Inhalation of Nano-Objects and Their. https://standards.iteh.ai/catalog/standards/cen/530459e6-1cf8-4f7b-9d0f-00aa48b687a5/en-17058-2018.

Fadeel, B., Bussy, C., Merino, S., Vázquez, E., Flahaut, E., Mouchet, F., Evariste, L., Gauthier, L., Koivisto, J., Vogel, U., Martín, C., Delogu, L.G., Buerki-Thurnherr, T., Wick, P., Beloin-Saint-Pierre, D., Hischier, R., Pelin, M., Carniel, F.C., Tretiach, M., Cesca, F., Benfenati, F., Scaini, D., Ballerini, L., Kostarelos, K., Prato, M., Alberto Bianco, A., 2018. Safety assessment of graphene-based materials: focus on human health and the environment. ACS Nano 12, 10582–10620. https://doi.org/10.1021/acsnano.8b04758.

Furxhi, I., Koivisto, A.J., Murphy, F., Trabucco, S., Del Secco, B., Arvanitis, A., 2021. Data shepherding in nanotechnology. The exposure field campaign template. Nanomaterilas 11, 1818. https://doi.org/10.3390/nano11071818.

Furxhi, I., Perucca, M., Blosi, M., Lopez De Ipiña, J., Oliveira, J., Murphy, F., Luisa Costa, A., Corsi, I., George, S., Koumoulos, E.P., Som, C., 2022. ASINA project: towards a methodological data-driven sustainable and safe-by-design approach for the development of nanomaterials. Front Bioeng Biotechnol 9, 805096. https://doi.org/10.3389/fbioe.2021.805096.

Geiss, O., Bianchi, I., Barrero-Moreno, J., 2016. Lung-deposited surface area concentration measurements in selected occupational and non-occupational environments. J. Aerosol Sci. 96, 24–37. https://doi.org/10.1016/J. JAEROSCI.2016.02.007.

Gupta, A., Silver, S., 1998. Silver as a biocide: will resistance become a problem? Nat. Biotechnol. 16, 888. https://doi.org/10.1038/nbt1098-888.

Iavicoli, I., Fontana, L., Pingue, P., Todea, A.M., Asbach, C., 2018. Assessment of occupational exposure to engineered nanomaterials in research laboratories using personal monitors. Sci. Total Environ. 627, 689–702. https://doi.org/10.1016/J. SCITOTENV.2018.01.260.

Koivisto, A.J., Aromaa, M., Mä, J.M., Pasanen, P., Hussein, T., Hä, K., 2011. Concept to estimate regional inhalation dose of industrially synthesized nanoparticles. ACS Nano 6 (2), 1195–1203. https://doi.org/10.1021/nn203857p.

Koivisto, A.J., Kling, K.I., Levin, M., Fransman, W., Gosens, I., Cassee, F.R., Jensen, K.A., 2017. First order risk assessment for nanoparticle inhalation exposure during injection molding of polypropylene composites and production of tungsten-carbide-cobalt fine powder based upon pulmonary inflammation and surface area dose. NanoImpact 6, 30–38. https://doi.org/10.1016/J.IMPACT.2016.11.002.

Koivisto, A.J., del Secco, B., Trabucco, S., Nicosia, A., Ravegnani, F., Altin, M., Cabellos, J., Furxhi, I., Blosi, M., Costa, A., Lopez De Ipiña, J., Belosi, F., 2022. Quantifying emission factors and setting conditions of use according to ECHA chapter R.14 for a spray process designed for nanocoatings-a case study. Nanomaterials 12, 596. https://doi.org/10.3390/nano12040596.

Kuempel, E.D., Attfield, M.D., Stayner, L.T., Castranova, V., 2014. Human and animal evidence supports lower occupational exposure limits for poorly-soluble respirable particles letter to the editor re: "low-toxicity dusts: current exposure guidelines are not sufficiently protective" by. Ann. Occup. Hyg. 58, 1205–1208. https://doi.org/10.1093/annhyg/meu058.

Lee, S.Y., Park, S.J., 2013. TiO2 photocatalyst for water treatment applications. J. Ind. Eng. Chem. 19, 1761–1769. https://doi.org/10.1016/J.JIEC.2013.07.012.

Nel, A., Xia, T., Mädler, L., Li, N., 2006. Toxic potential of materials at the Nanolevel. Science 311, 622–627. https://doi.org/10.1126/science.1114397.

Nicosia, A., Manodori, L., Trentini, A., Ricciardelli, I., Bacco, D., Poluzzi, V., Di Matteo, L., Belosi, F., 2018. Field study of a soft X-ray aerosol neutralizer combined with electrostatic classifiers for nanoparticle size distribution measurements. Particuology 37, 99–106. https://doi.org/10.1016/j.partic.2017.08.001.

NIOSH, 2011. Current intelligence bulletin 63: occupational exposure to titanium dioxide. In: National Institute for Occupational Safety and Health. Department of Health and Human Services. Public Health Service. Centers for Disease Control and Prevention. https://doi.org/10.26616/NIOSHPUB2011160. NIOSH Publication No. 2011–160.

NIOSH, 2021. In: Kuempel, E., Roberts, J.R., Roth, G., Dunn, K.L., Zumwalde, R., Drew, N., Hubbs, A., Trout, D., Holdsworth, G. (Eds.), Current Intelligence Bulletin 70: Health Effects of Occupational Exposure to Silver Nanomaterials. U.S. Department of Health and Human Services, Centers for Disease Control and Prevention, National Institute for Occupational Safety and Health, DHHS (NIOSH) Publication No. 2021-112, Cincinnati, OH. https://doi.org/10.26616/NIOSHPUB2021112.

Noël, A., Truchon, G., Cloutier, Y., Charbonneau, M., Maghni, K., Tardif, R., 2017. Mass or total surface area with aerosol size distribution as exposure metrics for inflammatory, cytotoxic and oxidative lung responses in rats exposed to titanium dioxide nanoparticles. Toxicol. Ind. Health 33, 351–364. https://doi.org/10.1177/0748233716651560/ASSET/IMAGES/LARGE/10.1177_0748233716651560-FIG2.JPEG.

Oberbek, P., Kozikowski, P., Czarnecka, K., Sobiech, P., Jakubiak, S., Jankowski, T., 2019. Inhalation exposure to various nanoparticles in work environment—contextual information and results of measurements. J. Nanopart. Res. 21, 1–24. https://doi.org/10.1007/S11051-019-4651-X/TABLES/6.

Oberdörster, G., Oberdörster, E., Oberdörster, J., 2005. Nanotoxicology: an emerging discipline evolving from studies of ultrafine particles. Environ. Health Perspect. 113, 823–839. https://doi.org/10.1289/EHP.7339.

Ortelli, S., Belosi, F., Bengalli, R., Ravegnani, F., Baldisserri, C., Perucca, M., Azoia, N., Blosi, M., Mantecca, P., Costa, A.L., 2020. Influence of spray-coating process parameters on the release of TiO2 particles for the production of antibacterial textile. NanoImpact 19, 100245. https://doi.org/10.1016/J.IMPACT.2020.100245.

Saber, A.T., Jacobsen, N.R., Jackson, P., Poulsen, S.S., Kyjovska, Z.O., Halappanavar, S., Yauk, C.L., Wallin, H., Vogel, U., 2014. Particle-induced pulmonary acute phase response may be the causal link between particle inhalation and cardiovascular disease. Wiley Interdiscip Rev Nanomed Nanobiotechnol 6, 517–531. https://doi.org/10.1002/WNAN.1279.

Salmatonidis, A., Ribalta, C., Sanfélix, V., Bezantakos, S., Biskos, G., Vulpoi, A., Simion, S., Monfort, E., Viana, M., 2019. Workplace exposure to nanoparticles during thermal spraying of ceramic coatings. Ann Work Expo Health 63, 91–106. https://doi.org/10.1093/ANNWEH/WXY094.

Santi, E., Belosi, F., Santachiara, G., Prodi, F., Berico, M., 2010. Real-time aerosol photometer and optical particle counter comparison. Il Nuovo Cimento B 125, 969–981. https://doi.org/10.1393/ncb/i2010-10904-5.

Schmid, O., Stoeger, T., 2016. Surface area is the biologically most effective dose metric for acute nanoparticle toxicity in the lung. J. Aerosol Sci. 99, 133–143. https://doi.org/10.1016/J.JAEROSCI.2015.12.006.

Schulte, P.A., Murashov, V., Zumwalde, R., Kuempel, E.D., Geraci, C.L., 2010. Occupational exposure limits for nanomaterials: state of the art. J. Nanopart. Res. 12, 1971–1987. https://doi.org/10.1007/s11051-010-0008-1.

Thompson, J.C., Wilson, P.G., Shridas, P., Ji, A., de Beer, M., de Beer, F.C., Webb, N.R., Tannock, L.R., 2018. Serum amyloid A3 is pro-atherogenic. Atherosclerosis 268, 32–35. https://doi.org/10.1016/J.ATHEROSCLEROSIS.2017.11.011.

Trabucco, S., Ortelli, S., del Secco, B., Zanoni, I., Belosi, F., Ravegnani, F., Nicosia, A., Blosi, M., Costa, A.L., 2021. Monitoring and optimisation of ag nanoparticle spray-coating on textiles. Nanomaterials 11, 3165. https://doi.org/10.3390/nano11123165.

van Rijn, J., Afantitis, A., Culha, M., Dusinska, M., Exner, T.E., Jeliazkova, N., Longhin, E.M., Lynch, I., Melagraki, G., Nymark, P., Papadiamantis, A.G., Winkler, D.A., Yilmaz, H., Willighagen, E., 2022. European registry of materials: global, unique identifers for (undisclosed) nanomaterials. J. Cheminformat. 14, 57. https://doi.org/10.1186/s13321-022-00614-7.

WHO, 2017. WHO Guidelines on Protecting Workers from Potential Risks of Manufactured Nanomaterials, 85 pp. ISBN: 9789241550048.

Wu, T.Y., Horender, S., Tancev, G., Vasilatou, K., 2022. Evaluation of aerosol-spectrometer based PM2.5 and PM10 mass concentration measurement using ambient-like model aerosols in the laboratory. Measurement 201, 111761. https://doi.org/10.1016/J.MEASUREMENT.2022.111761.